NSTX-U

Supported by

U.S. DEPARTMENT OF ENERGY | Office of Science

Modification of impurity transport and divertor sources due to lithium wall conditioning in NSTX

Filippo Scotti

Princeton Plasma Physics Laboratory

Oak Ridge National Laboratory
Fusion Energy Science & Technology Seminar
November 25th , 2013

Coll of Wm & Mary
Columbia U
CompX
General Atomics
FIU
INL
Johns Hopkins U
LANL
LLNL
Lodestar
MIT
Lehigh U
Nova Photonics
ORNL
PPPL
Princeton U
Purdue U
SNL
Think Tank, Inc.
UC Davis
UC Irvine
UCLA
UCSD
U Colorado
U Illinois
U Maryland
U Rochester
U Tennessee
U Tulsa
U Washington
U Wisconsin
X Science LLC

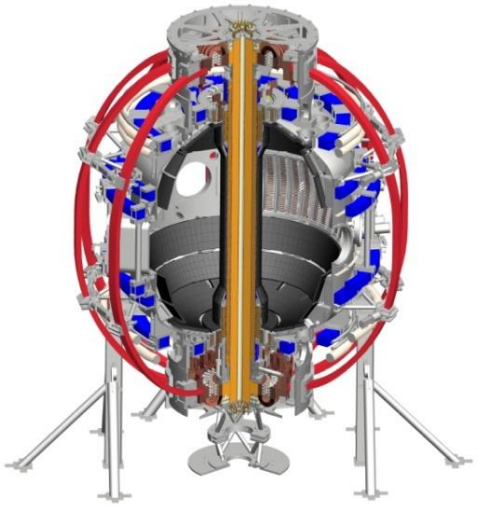

Culham Sci Ctr
York U
Chubu U
Fukui U
Hiroshima U
Hyogo U
Kyoto U
Kyushu U
Kyushu Tokai U
NIFS
Niigata U
U Tokyo
JAEA
Inst for Nucl Res, Kiev
Ioffe Inst
TRINITI
Chonbuk Natl U
NFRI
KAIST
POSTECH
Seoul Natl U
ASIPP
CIEMAT
FOM Inst DIFFER
ENEA, Frascati
CEA, Cadarache
IPP, Jülich
IPP, Garching
ASCR, Czech Rep

Evaporative lithium coatings routinely applied on NSTX plasma facing components for wall conditioning

- Graphite is the main PFC material in NSTX:
  - ATJ tiles on divertor and outer wall
  - ATJ and CFC tiles on center stack
  - Porous moly in outer divertor (LLD)
- Lithium coatings evaporated on PFCs [1]:
  - 100–300 mg of lithium applied between discharges using evaporators (LITERs)
  - Nominal "coating" thickness ~20-40 nm (~10^{21} atoms/m^2)
- Highly toroidally asymmetric deposition

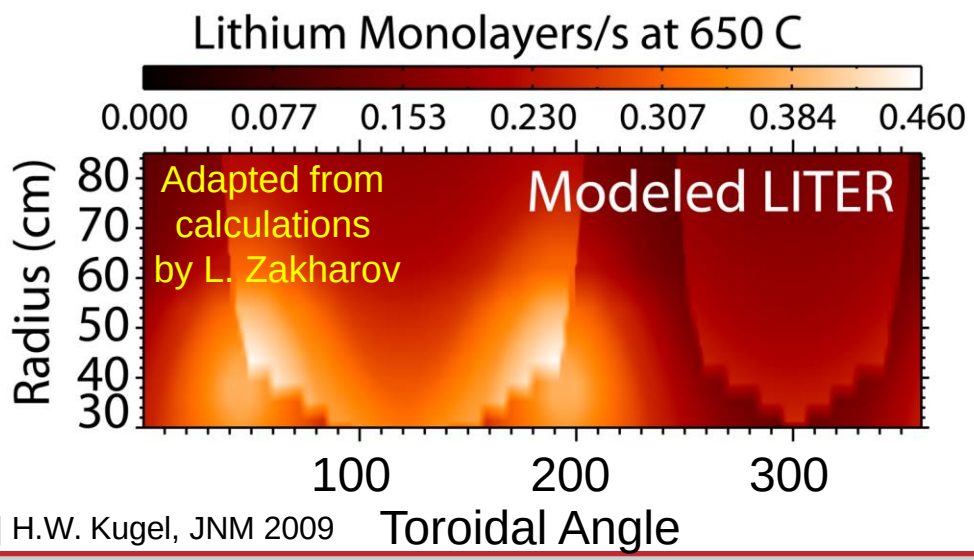

[1] H.W. Kugel, JNM 2009

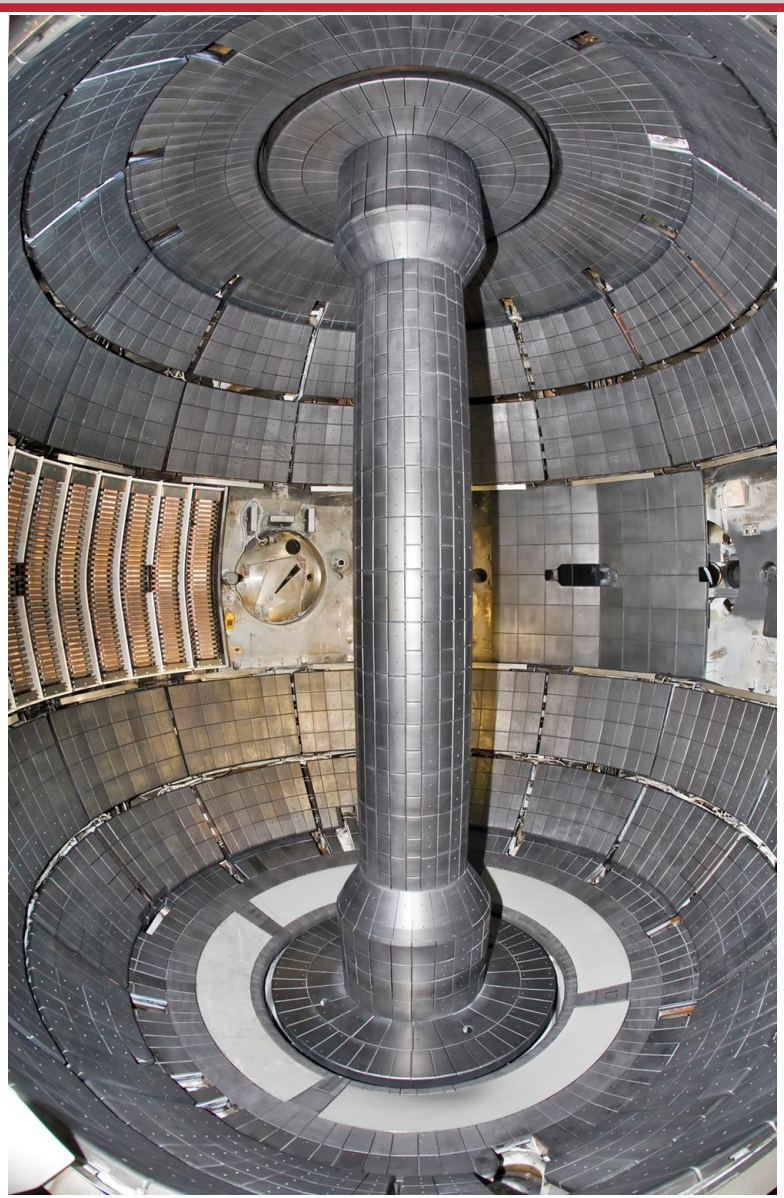

Wall conditioning via lithium evaporative coatings on graphite in NSTX resulted in impurity accumulation

- Benefits observed with lithium conditioning:
  - reduction in deuterium wall recycling
    - re-attachment of inner divertor, disappearance of MARFE [1]
  - deuterium inventory control
    - via reduced recycling [2]
  - increase in energy confinement time
    - reduced transport at lower ν^*_e [3,4]
  - suppression of ELMs
    - due to changes in n_e profiles [5]
- However:
  - carbon inventory increased by 3-4X [6]
  - high-Z impurity accumulation leads to core P_{rad} up to 50% of P_{inj} [7]
  - low core lithium density (n_{Li}/n_e<0.1%) [8]

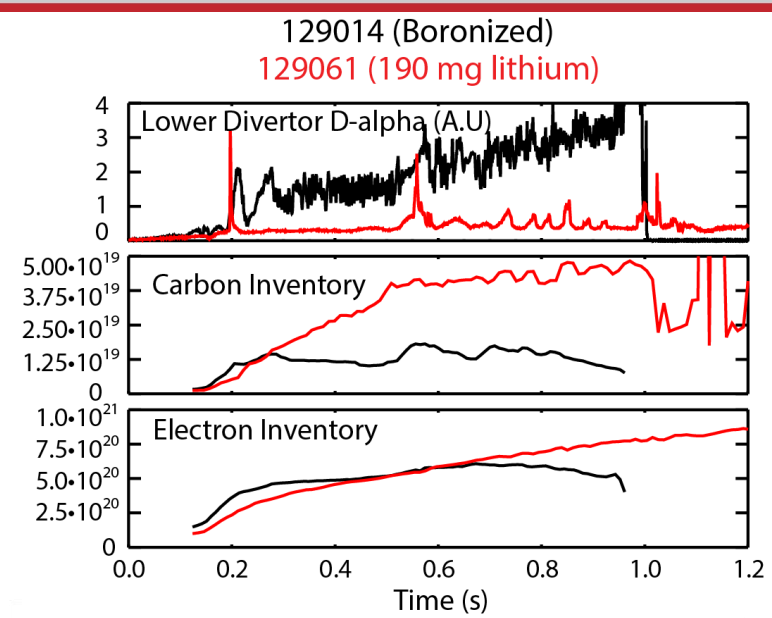

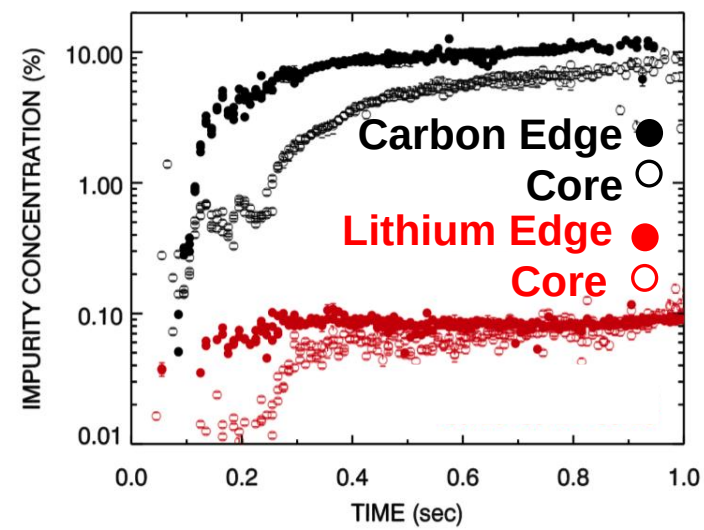

[1] F. Scotti, JNM 2011.
[2] V.A. Soukhanovskii, IAEA 2010.
[3] S.M. Kaye, NF 2013.
[4] J.M. Canik, NF 2013.
[5] R. Maingi, NF 2013.
[6] F. Scotti, NF 2013.
[7] S.F. Paul, JNM 2009.
[8] M. Podesta, NF 2012.

Outline: lithium conditioning affects divertor impurity influxes, SOL transport, and core transport

- Divertor impurity influxes:
  - Lithium sputtering consistent with physical sputtering from solid/liquid lithium coatings
  - Moderate reduction in carbon sputtering yield
- SOL parallel transport:
  - Stronger divertor retention for lithium than carbon
  - Retention weakens at reduced target recycling
- Core & edge radial transport:
  - Increase in carbon inventories mostly due to disappearance of ELMs
  - High neoclassical diffusivity helps prevent lithium accumulation

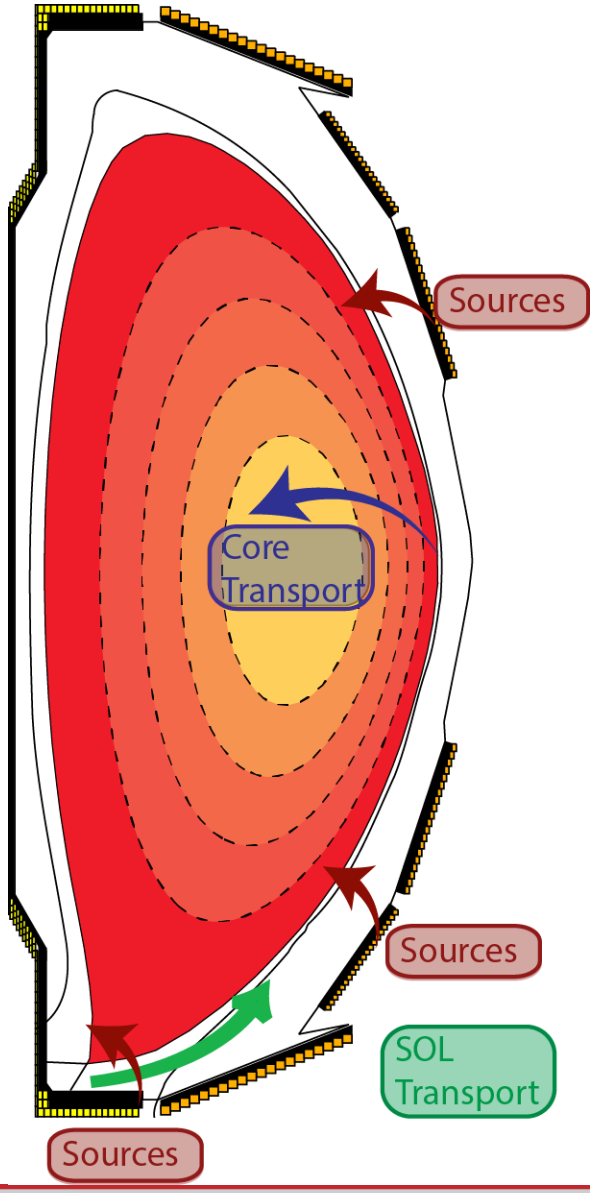

NSTX diagnostics are well suited for divertor impurity influxes and core transport studies

- Spectroscopic diagnostics for divertor impurity influxes:
  - divertor spectrometer (C II,CD) [1,2], 1D/2D cameras (Li I-II,C II-IV) [3]
  - S/XB method

$$\Gamma_i = \frac{S}{X\ B}\ \Gamma_{ph}$$

- Langmuir probes for T_e, n_e, J_{sat} [4]

$$Y = \frac{\Gamma_{imp}}{\Gamma_{D+}} = \frac{\Gamma_{ph-imp} S / XB_{imp}}{J_{SAT}}$$

- IR thermography for divertor T_{surf} [5]
- Midplane kinetic profiles measured by:
  - CHarge Exchange Recombination Spectroscopy (CHERS) : T_i, v_{tor}, n_C, n_{Li} (51 points, 10 ms resolution) [6,7]
  - Thomson scattering: T_e, n_e, (30 points, 30 ms resolution) [8]

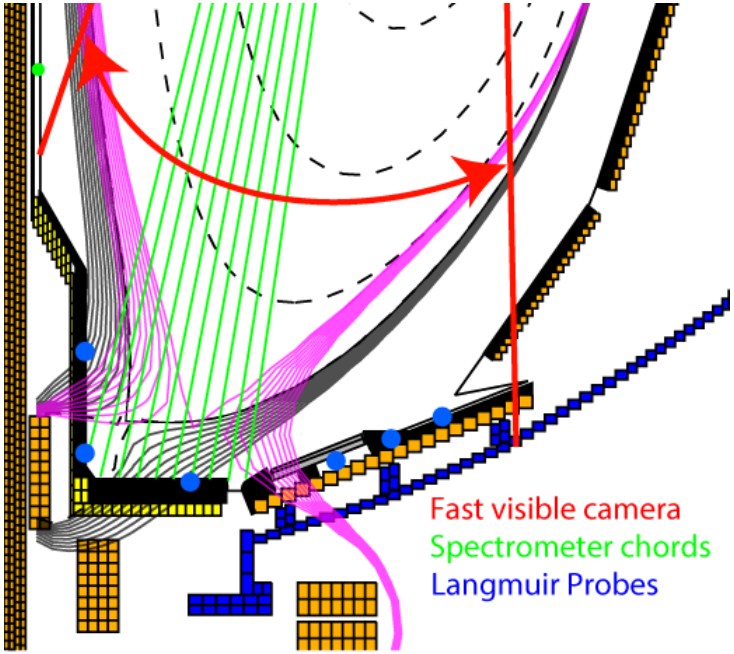

[1,2] V.A. Soukhanovskii, RSI 2006, 2010.
[3] F. Scotti, RSI 2012.
[4] J.B. Kallman, RSI 2010.
[5] A.G. McLean, RSI 2012.
[6] R.E. Bell, RSI 2010.
[7] M. Podesta, NF 2012.
[8] B.P. LeBlanc, RSI 2003.

2D fast divertor cameras installed for studies of impurity influxes, non-axisymmetric PMI and divertor monitoring

- Two 2D divertor fast divertor camera systems [1]:
  - full toroidal coverage: re-entrant port, coherent fiber bundle, low aspect ratio of ST
  - spatial resolution of 0.8 cm/pixel, frame rate of 100 kHz (256 x 208 pixels)
  - 12-14 bit dynamic range (Phantom 710, 7.3)
  - narrow bandpass filters on remotely controlled filter wheel
- 2D spatial and absolute photometric calibration:
  - whiteplate and Labsphere calibration
- Custom toroidal remapping
  - easier analysis of non-axisymmetric effects

[1] F. Scotti, RSI 2012.

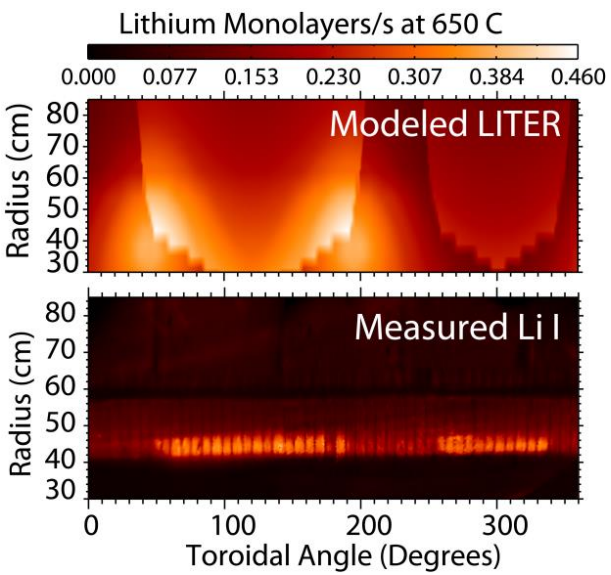

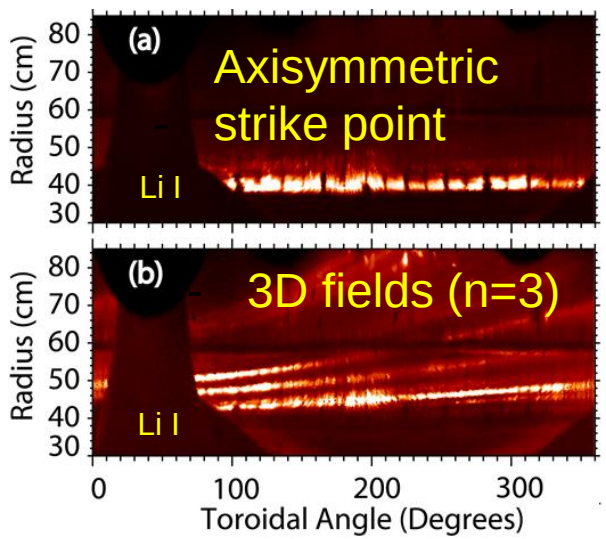

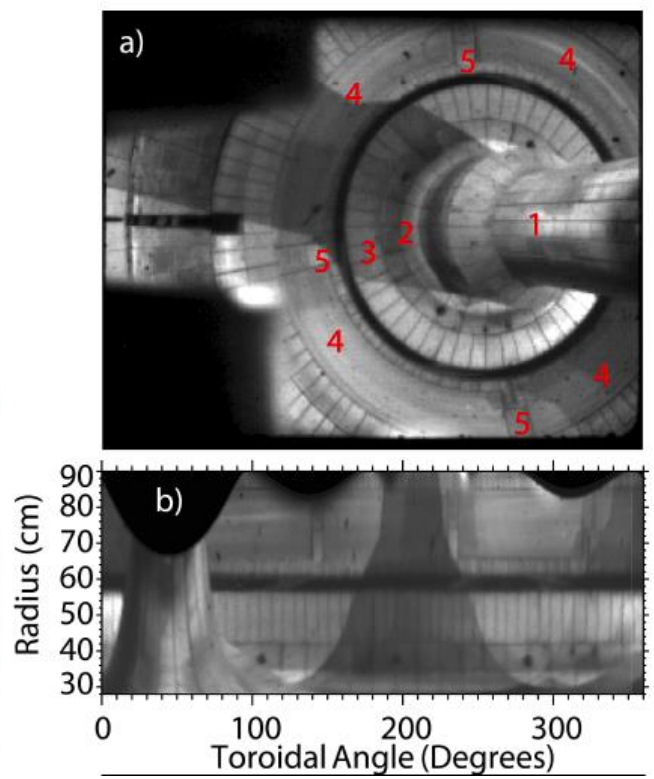

Divertor impurity influxes are analyzed in discharges with boronized and lithiated PFCs

Divertor impurity influxes:

- Carbon:
  - Boronized vs lithiated discharges
- Carbon and Lithium:
  - Lithiated discharges

SOL parallel transport:

- Carbon and lithium
  - Lithiated discharges

Core & edge radial transport:

- Carbon:
  - Boronized vs lithiated discharges
- Carbon and lithium
  - Lithiated discharges

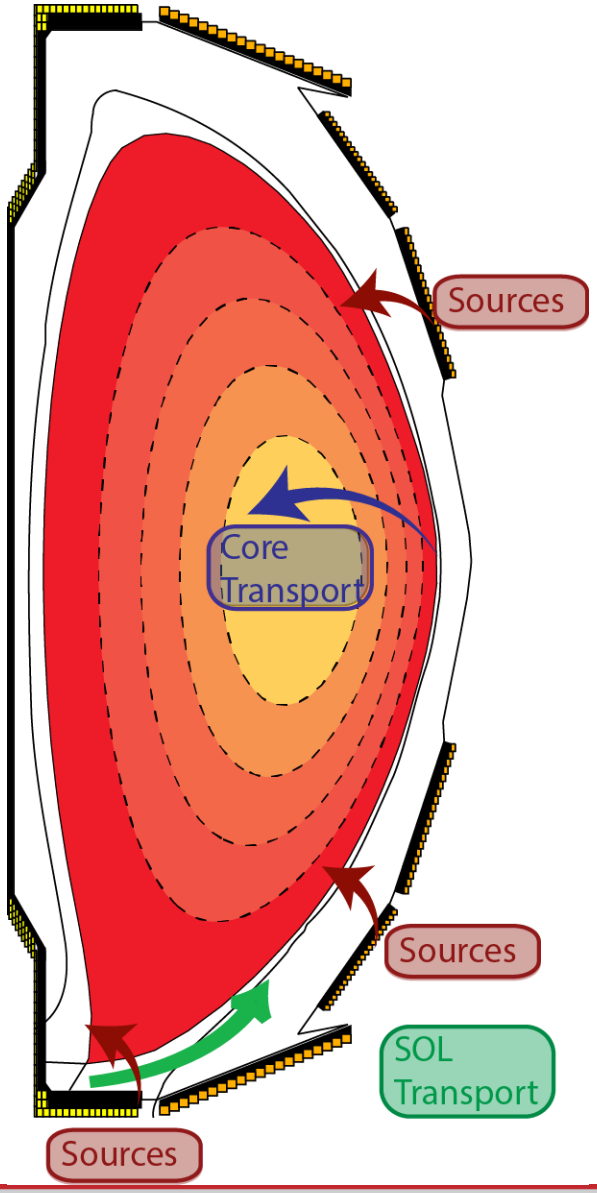

“Thermal” lithium sputtering yield is expected to be the dominant lithium sputtering mechanism in NSTX divertor

- Physical sputtering is the main lithium sputtering process
  - Threshold energy E_{th} ~10 eV, 2/3 sputtered as ions
- “Thermal” sputtering (T_m=180ºC) observed in test stands (PISCES, IIAX)
  - Dominates lithium influxes for T_{surf} < 550ºC for Γ_{D+}~10^{23} ions/m^2/s
- Carbon has physical (Y_{phys}, E_{th} ~30 eV) and chemical (Y_{chem}) sputt. processes
  - Y_{chem} dominates in low T_e plasmas, depends on incident flux and T_{surf}
- Reduction in Y_C on lithium-coated graphite observed in test stands (IIAX)
  - Associated to formation of ionic bonds between C - Li [Racic, JNM 2009]
  - Observed in MD simulations due to Li-C-O chemistry [Krstic, PRL 2013]

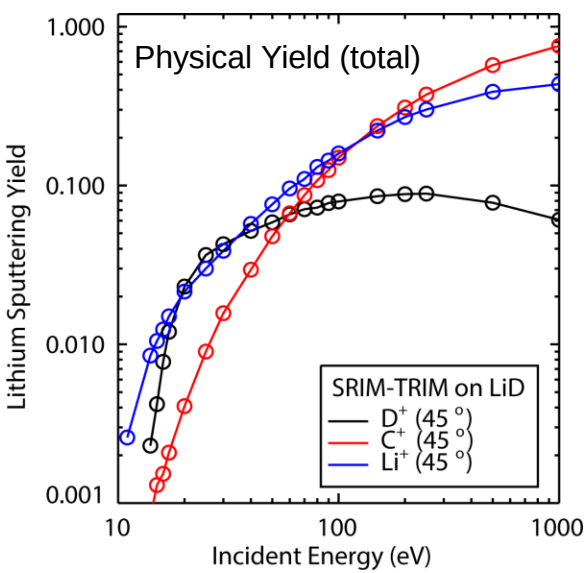

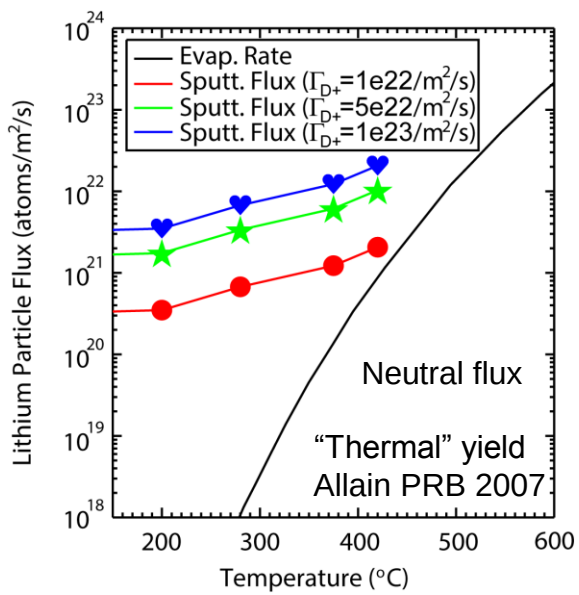

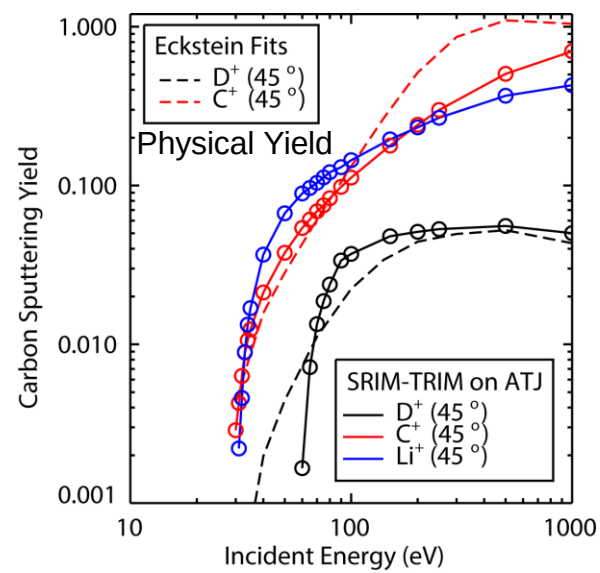

External and plasma heating of divertor PFCs allow study of thermal response of Y_{Li} in NSTX

- Discharges with unheated and externally heated PFCs (LLD):
  - after large evaporation (~200 g) nominal "coating" thickness ~10s μm
  - outer strike point at R ~ 62 cm
- Differential heating of LLD leads to non-axisymmetric lithium influxes:
  - 3 LLD plates externally heated to 250ºC only in one discharge
  - enhancement consistent with expectations from T_{surf} enhanced Y_{Li}
- Asymmetries observed also at strike point as a result of plasma heating
  - follow LITER deposition profile

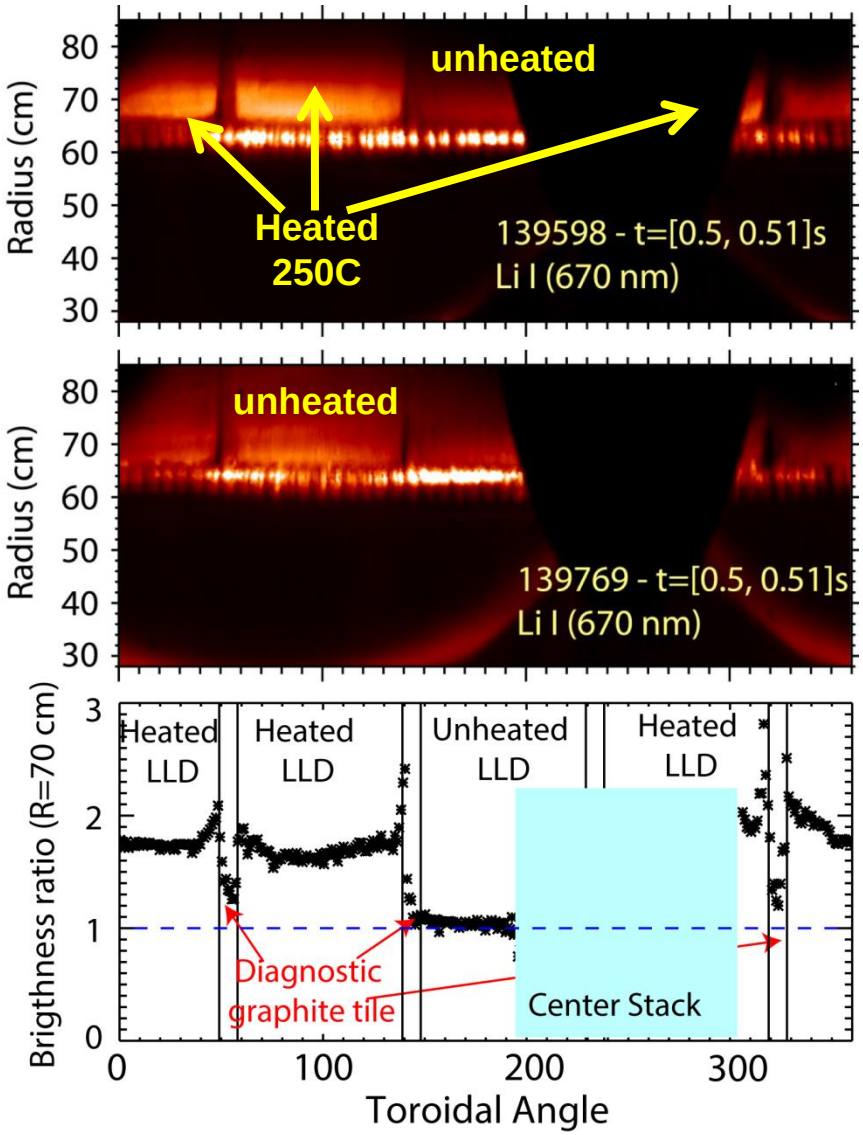

External and plasma heating of divertor PFCs allow study of thermal response of Y_{Li} in NSTX

- Discharges with unheated and externally heated PFCs (LLD):
  - after large evaporation (~200 g) nominal "coating" thickness ~10s μm
- Toroidal/radial locations analyzed:
  - Diagnostic graphite tile Φ ~ 145°
  - Cold LLD, Φ ~ 155°
  - Hot LLD, thick coatings Φ ~ 130°
  - Hot LLD, thin coatings Φ ~ 20°
  - R = [63, 64, 67, 70, 71, 72] cm

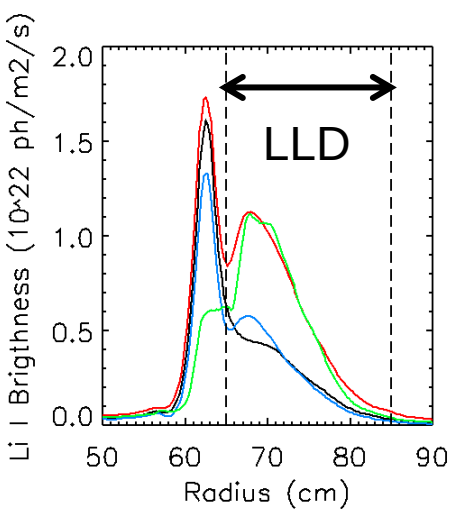

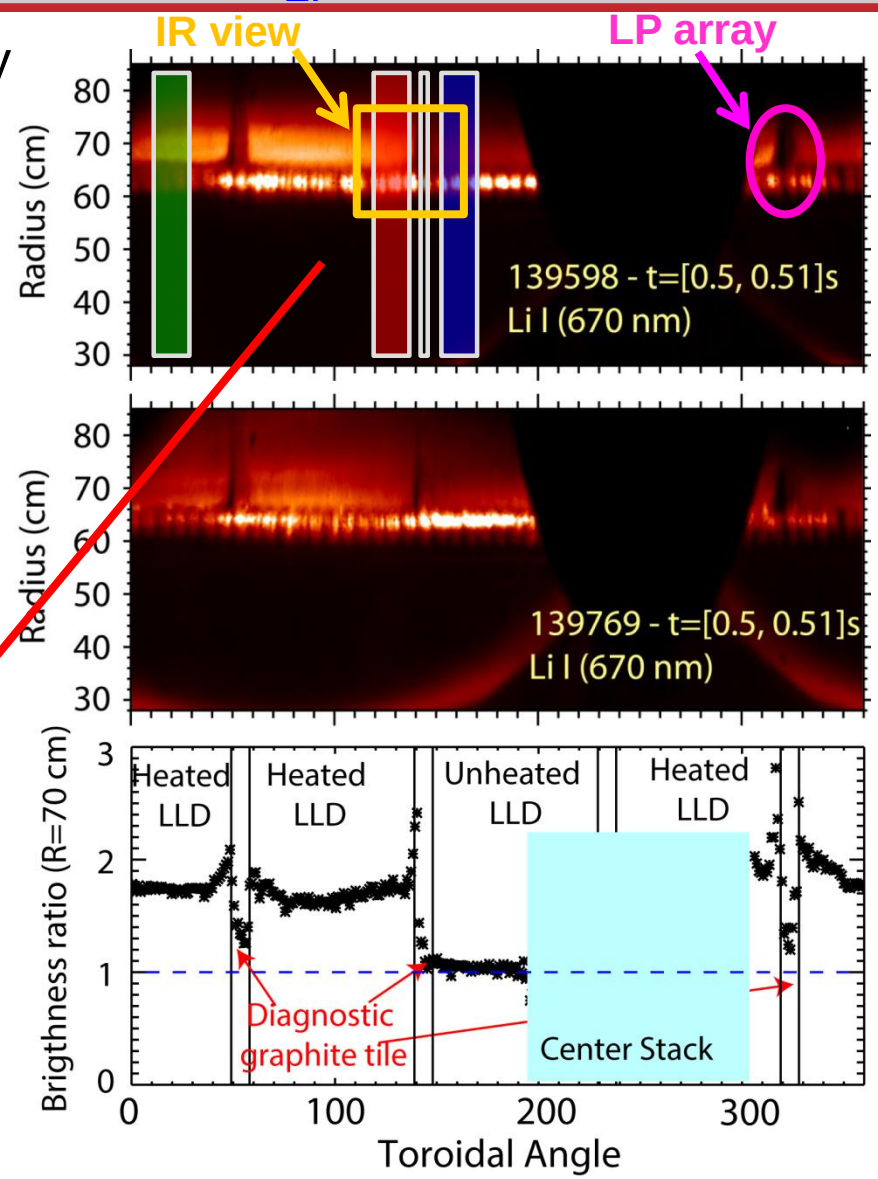

Temperature enhanced sputtering observed as a result of external and plasma heating of divertor target

- T_{surf} dependence of Y_{Li} observed as a result of external heating (up to 2X)
  - consistent with expected T_{surf}-dependence of Y_{Li}
  - comparable response from moly and graphite with thick lithium coatings
- Enhancement in sputtering yield at strike point only with thick coatings

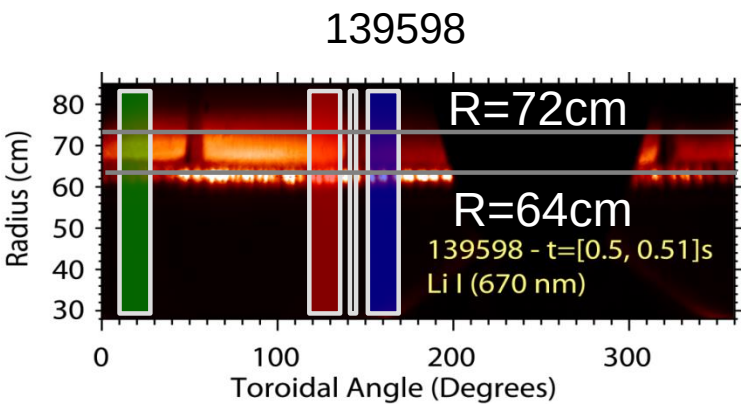

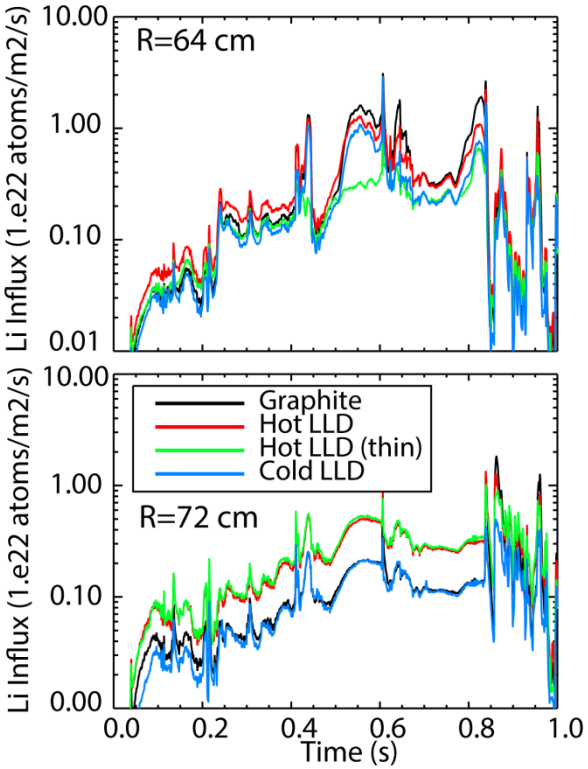

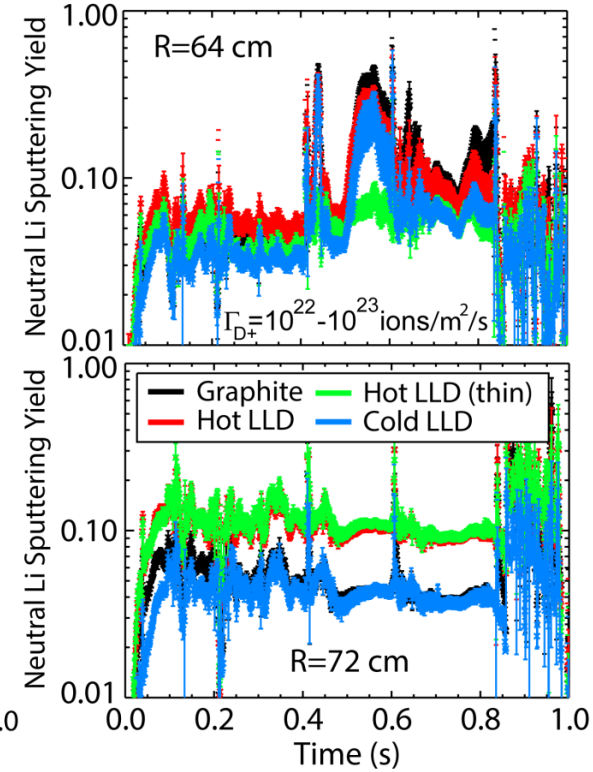

Experimental Y_{Li} consistent with physical sputtering with signature of T_{surf} dependent sputtering yield

- Y_{Li} from solid coatings consistent with SRIM-TRIM from LiD/Li (Y_{Li}~3-7%)
- Y_{Li} from liquid coatings consistent with "thermal" sputtering (Y_{Li}~10-20%)
  - Data averaged over 1 ms and 2-4º toroidally
  - Leading edge effects lead to variation of T_{surf} over graphite tile
  - Consistent results in several discharges (e.g. 139769 - Figure a)
- Transient anomalous enhancement of Y_{Li} at the OSP observed with fresh thick coatings (Figure b)
  - enhancement follows toroidal asymmetry in lithium deposition profile

139769
several discharges
after 200g evap

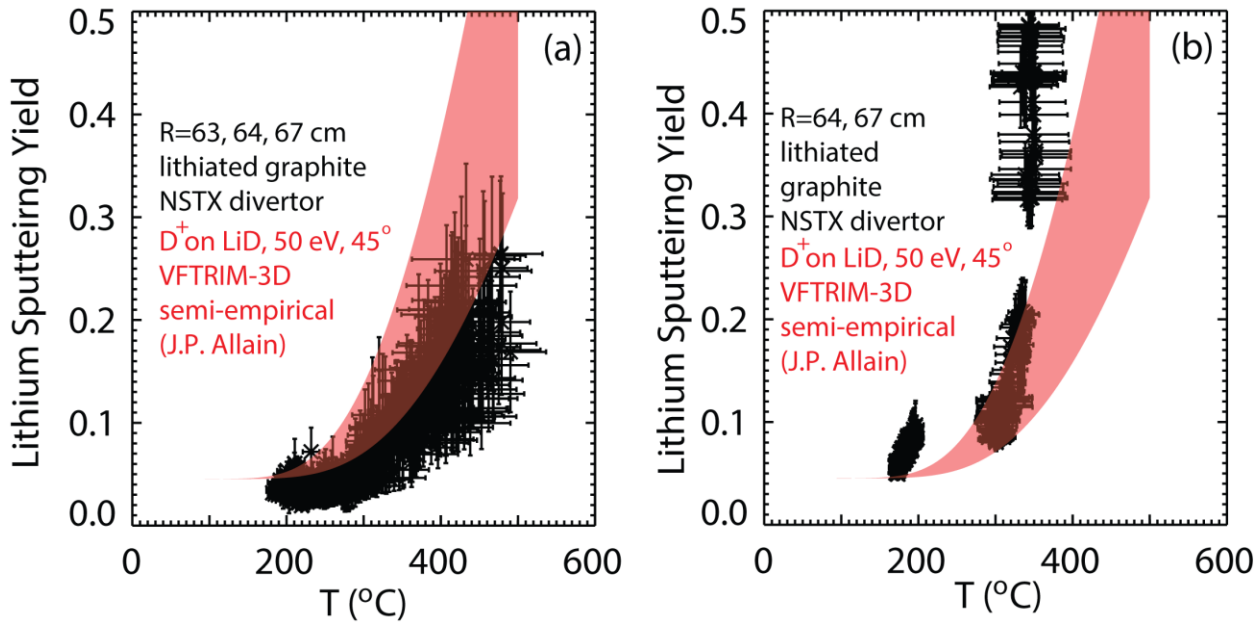

139598 –
fresh thick
coatings

Toroidal asymmetries in lithium influxes/sputtering yield observed closely following LITER deposition profile

- Anomalous transient Y_{Li} associated with toroidal asymmetries in lithium influxes
- Asymmetries occurring only close to the strike point
  - Closely follow LITER deposition profile
- Possibly associated with different thermal response, generation/ejection of lithium droplets, or degradation of lithium coatings
  - Not expected if lithium thickness > ion range

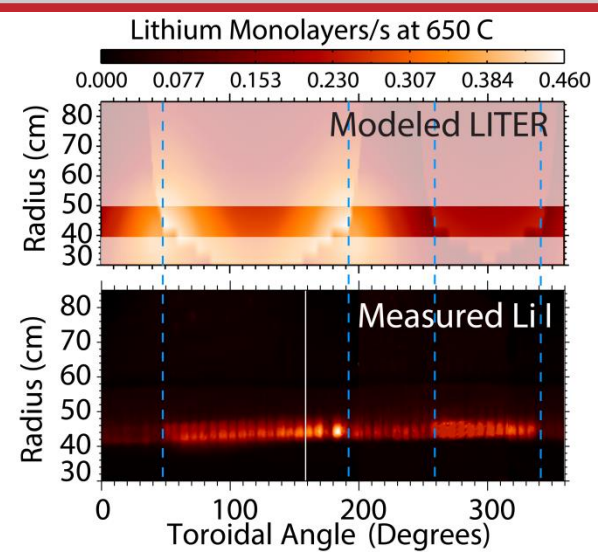

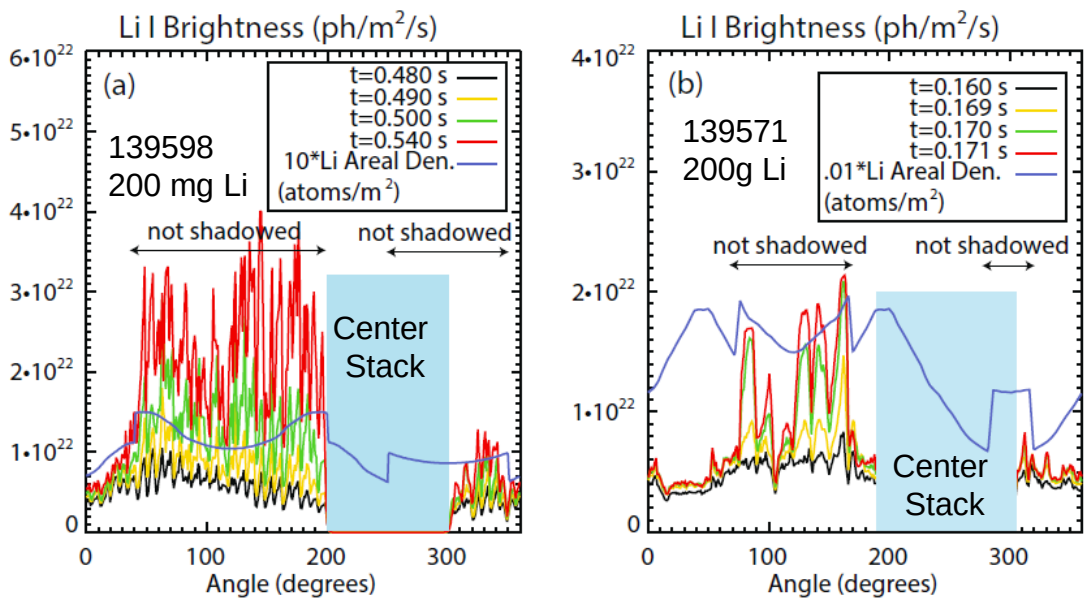

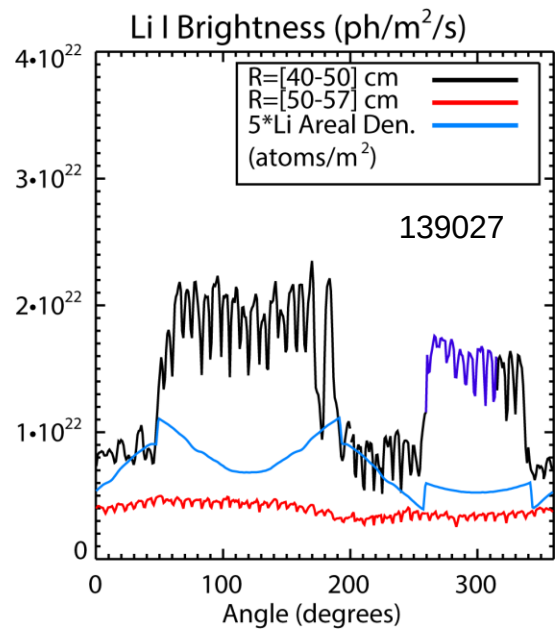

Moderate reduction in carbon sputtering yield in near/far SOL observed with lithium conditioning

- Carbon sputtering measured in near/far SOL with first evaporation of lithium on boronized graphite in 2008
- Reduction (2-3X) in C II-III emission from lower and upper divertor, and center stack
- Moderate reduction in sputtering yield (Y_C) with application of lithium:
  - Y_C from C II (VIPS2 at 392 nm): physical + chemical component
  - Complicated by T_e sensitivity of S/XB and ELM averaging
- Significant contribution from chemical sputtering:
  - From CD(430 nm)/D-γ vs C II(426 nm)/D-γ
  - Uncertainty in D/XB coefficients

Relative change in Y_C with lithium application

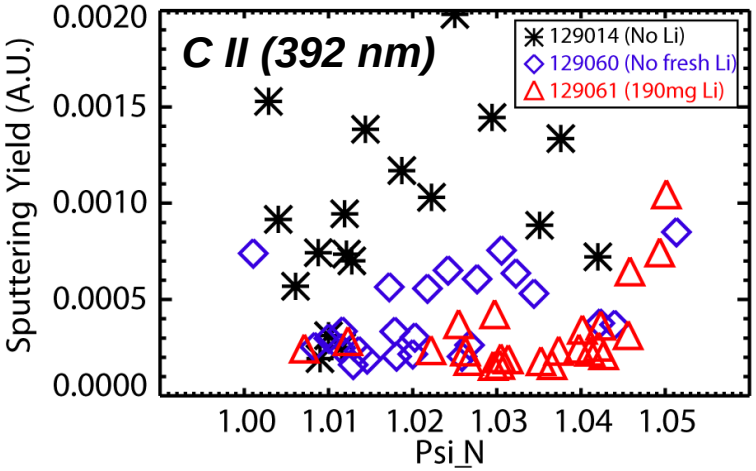

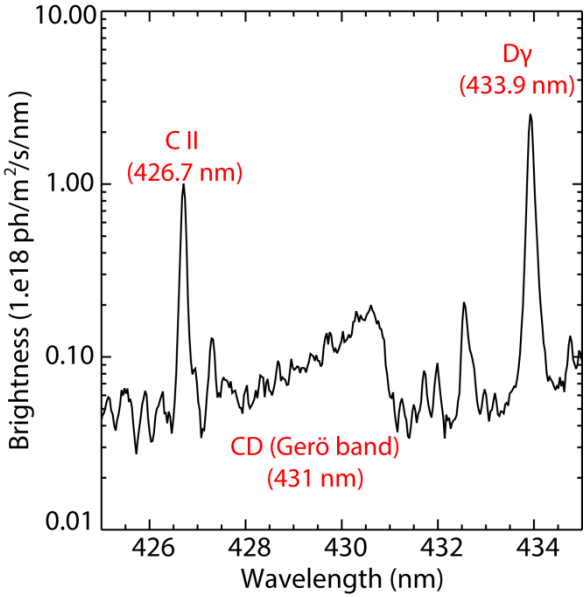

Measured Y_C on lithium conditioned graphite below estimates for physical and chemical sputtering

- In 2010, only lithium-coated divertor conditions:
  - Large set of 2D camera data: C II (658 nm), C III (465 nm), C IV (580 nm)

- Y_C near SOL reduced with respect to $Y_{phys}+Y_{chem}$ estimates [Eckstein+Roth]
  - Statistical analysis of 40 ELM-free H-modes
  - Y_{Chem} data from VIPS2 still need to be included in analysis

- However:
  - No clear dependence on amount of lithium
  - No increase in Y_C during discharge

- Y_C reduction from lithium coverage limited by:
  - Lifetime of coatings (intercalation, erosion)
  - Higher OSP T_e
  - Surface roughness >> "coating" thickness
  - Effect of tile leading edges
  - Migration of carbon from other sources

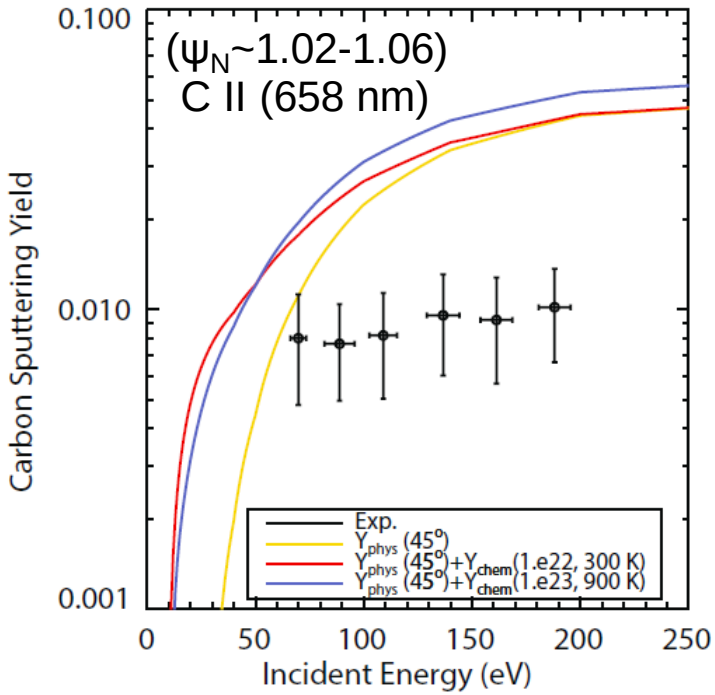

Upper estimate for penetration factor of divertor sources suggest stronger retention for lithium than carbon

- Poloidal distribution of impurity sources not understood
  - Upper divertor, wall sources not diagnosed
  - Study divertor influxes is one part of the problem
- OSP influxes from database using constant S/XBs:
  - Consistent influxes from C II, C III, C IV
    - $3\text{-}10\times10^{20}$ ions/s
  - Large neutral lithium divertor influxes
    - $1\text{-}6\times10^{21}$ atoms/s
  - Largely reduced (>x10) lithium ionized influxes
  - Suggest large re-deposition fraction ($\lambda_{mfpLi}<\rho_{Li}$)
- Core penetration factors for OSP sources fitting core particle inventories [McCracken, JNM 1997]
  - F ~10^{-4}-10^{-3} from Li I ; F~10^{-3}-10^{-2} from Li II
  - F ~1×10^{-1}-5×10^{-1} from C II

$$\frac{dN_Z(t)}{dt} = -\frac{N_Z(t)}{\tau_Z} + \sum_i F_i \Gamma_i,$$

$$N_Z(t) = F_i \exp\left(-\frac{t}{\tau_Z}\right) \int_0^t \Gamma_i(t) \exp\left(\frac{t}{\tau_Z}\right) dt.$$

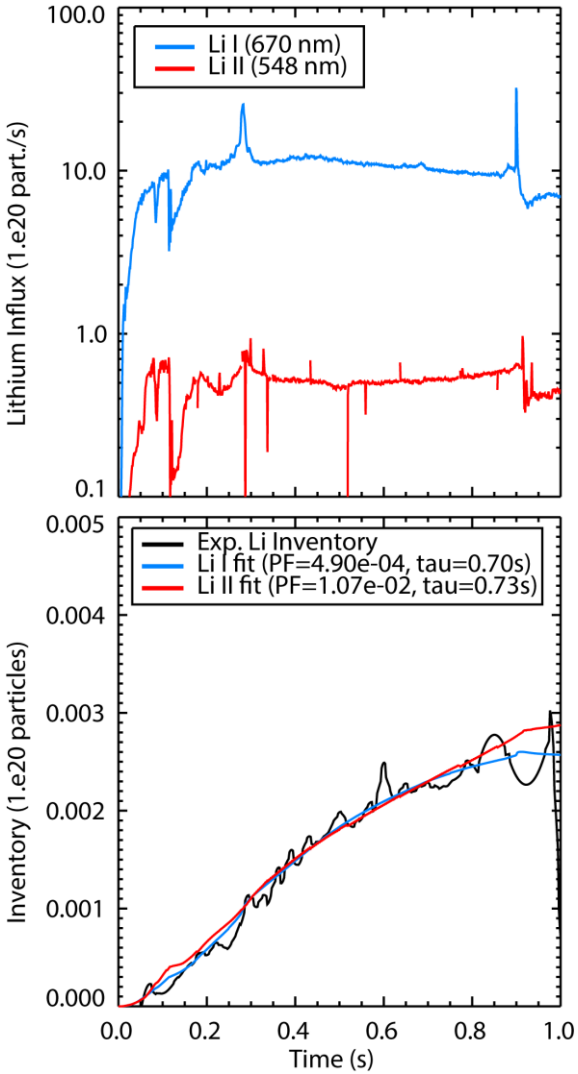

SOL parallel transport of sputtered atoms is analyzed to connect divertor influxes to core impurity content

Divertor impurity influxes:

- Moderate reduction in carbon sputtering with lithium conditioning
- Lithium sputtering consistent with physical sputtering

SOL parallel transport:

- Difference in carbon and lithium parallel transport

Core & edge radial transport:

- Carbon:
  - Boronized vs lithiated discharges
- Carbon and lithium
  - Lithiated discharges

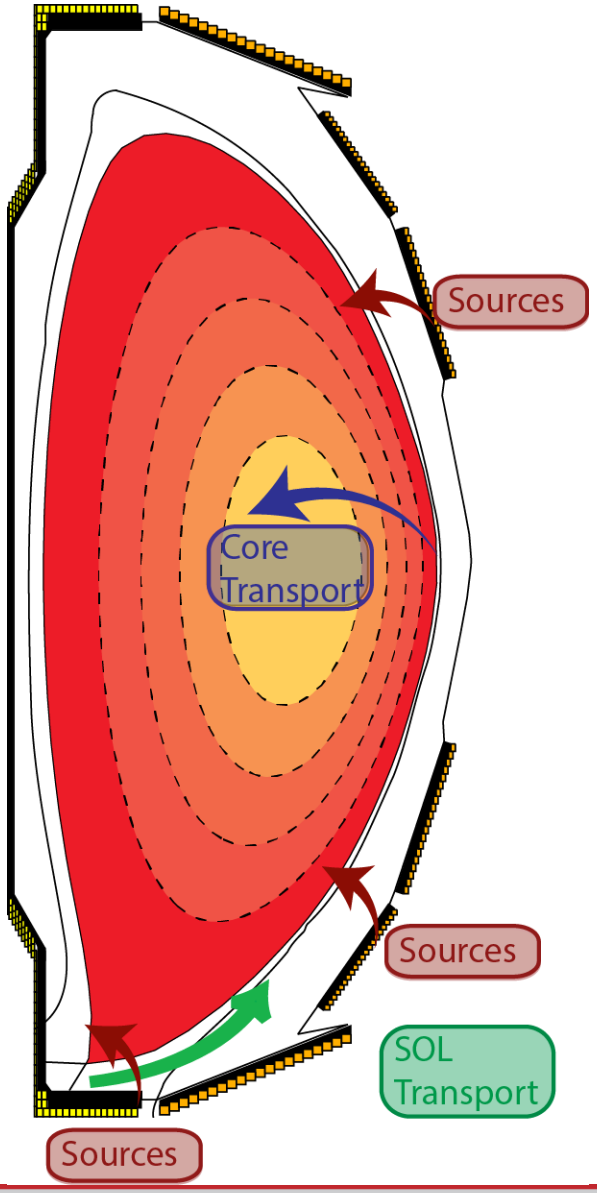

2D multi-fluid UEDGE simulations performed to investigate reasons for difference in penetration factors

- UEDGE, 2D multi-fluid edge code:
  - Fluid (Braginskii) model for D^0, D^+, e^-, C^{0-6+}, Li^{0-3+}
  - 20 radial, 60 poloidal cells
- Drifts not included in simulations:
  - In NSTX no SOL flows measurements
  - Classical parallel transport in exp. relevant conditions
- Radially varying main ion D_{perp}, χ_e, χ_i
  - Flux B.C. at core (64 A from NBI) + 500 A HFS puff
  - Core power B.C. (1.5+1.5 MW e,i)

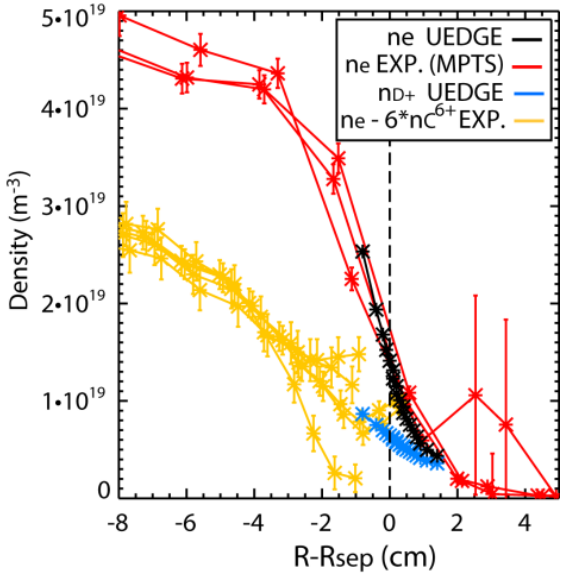

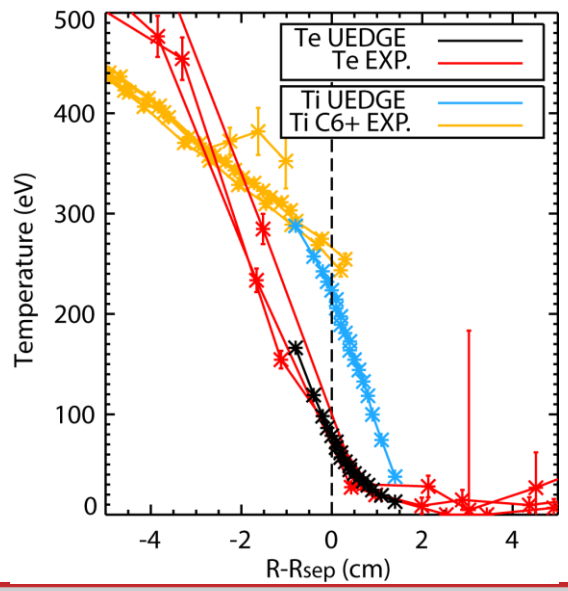

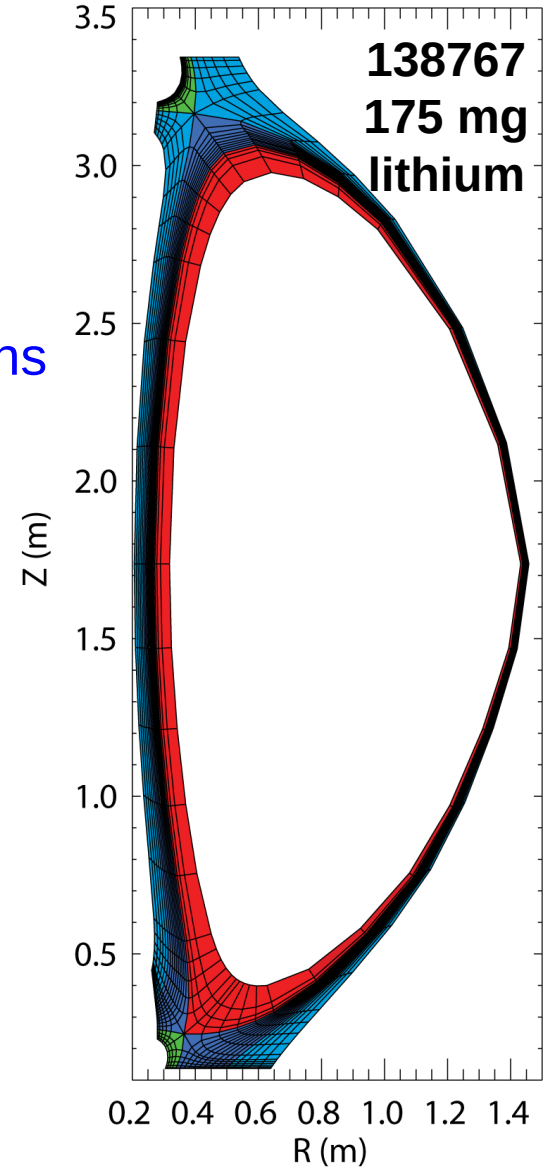

Charge state resolved model employed including lithium and carbon impurities

- Charge state resolved model for both carbon and lithium
  - Analytic solution of impurity parallel momentum equation
- Atomic rates from ADAS
  - Latest lithium rates from Auburn group [S. Loch, ADNDT 2006]
- Carbon and lithium radial transport
  - Radially uniform diffusivity for all charge states
  - Radially varying velocity for C^{6+}, Li^{3+} to match CHERS data
  - Core C^{1+}-C^{5+} (Li^{1+}-Li^{2+}) influx balanced by C^{6+} (Li^{3+}) outflux → zero net flux

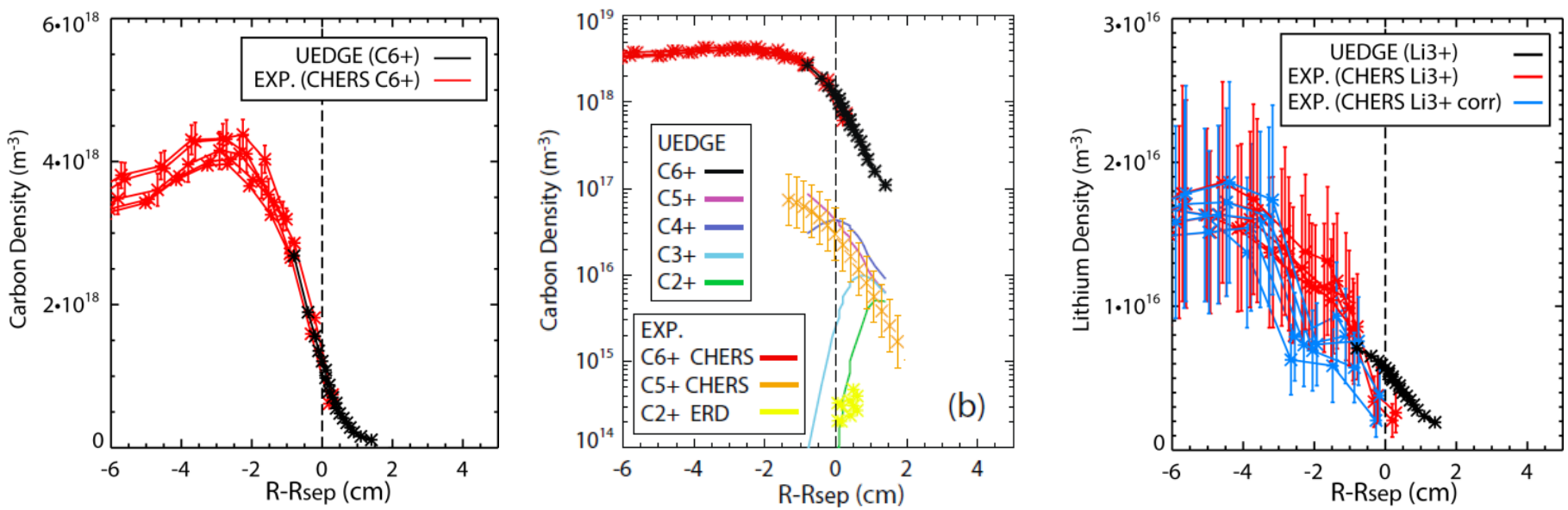

Recycling and impurity sputtering adjusted to match divertor heat flux, D-α, C II, Li II and particle balance

- Synthetic diagnostics used to reproduce experimental spectroscopic views
- Target recycling adjusted (R=0.95) to match strike point heat flux and D-α
- Carbon sputtering adjusted to match peak divertor C II
  - Haasz-Davis yield scaled by 0.4 at divertor → Y_C ~ 1%
  - Consistent with moderate reduction in Y_C with application of lithium
- Uniform lithium sputtering at target to match Li II
  - Cannot match Li I and Li II brightness for same Y_{Li}
- No effect on heat flux due to lithium radiation (even for 10X higher Y_{Li})
  - Divertor radiation still dominated by C and D

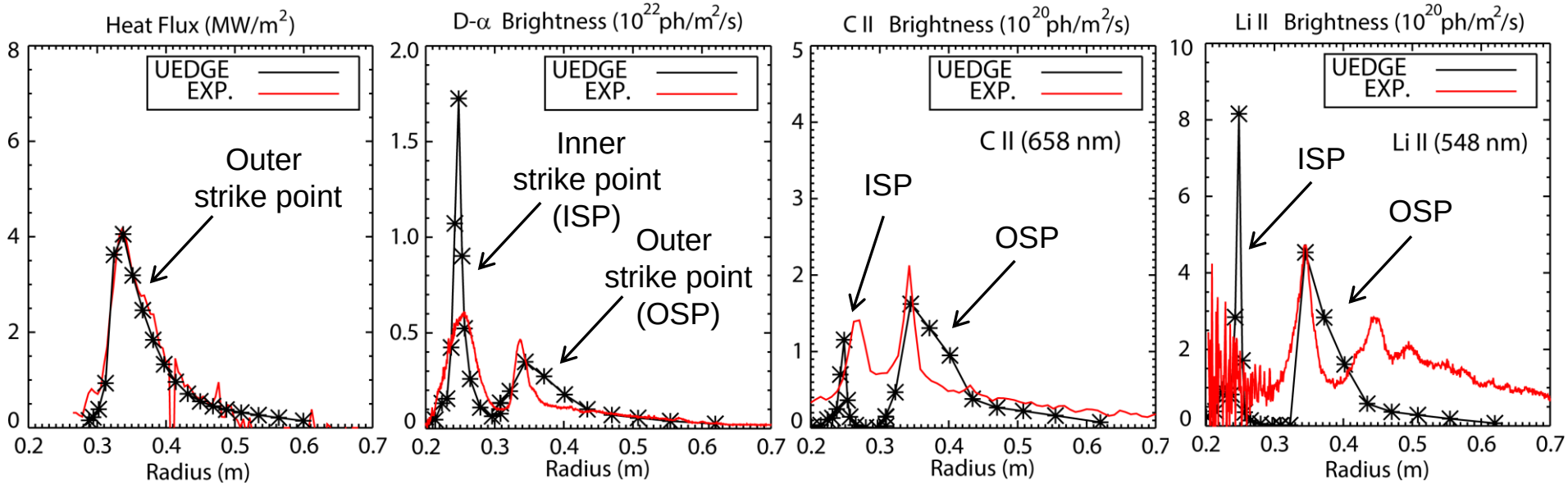

Difference in parallel impurity profiles observed between carbon and lithium in near target region and upstream

- Better divertor trapping of lithium ions with respect to carbon, weaker upstream pickup
- However, to match exp. lithium profiles higher perp. diffusivity was used for lithium with respect to carbon
  - Affects parallel impurity profiles, reducing upstream pickup
  - Even with $D_{Li}=D_C$, lower upstream contamination for lithium wrt carbon
- To address causes for differences in parallel transport, higher resolution slab simulations with same transport coefficients

Parallel impurity density profile
First SOL cell

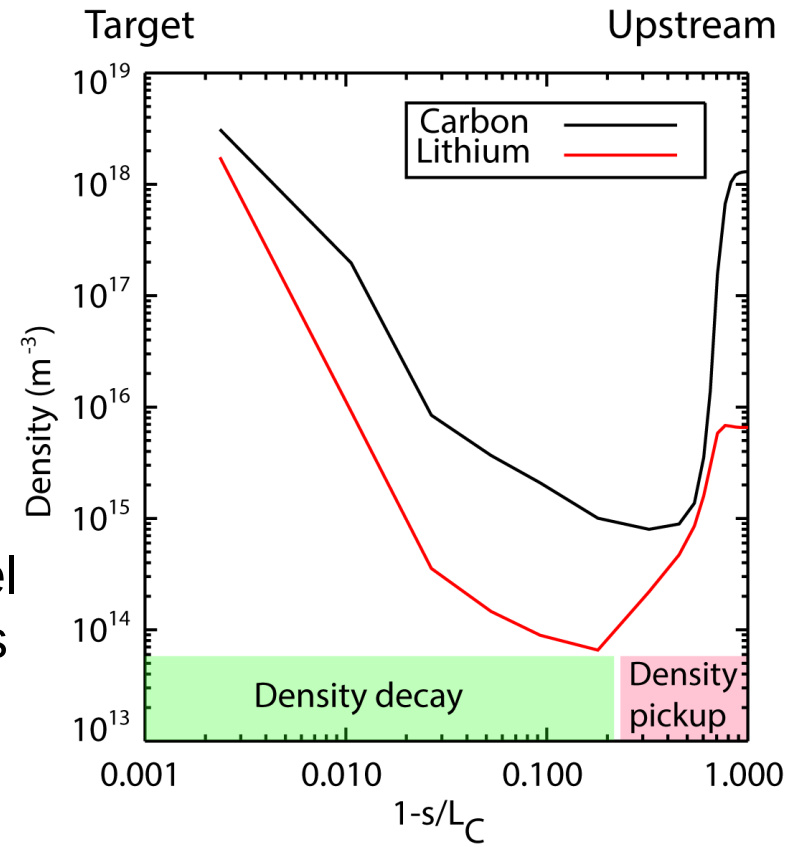

s distance from midplane
L_C midplane-target connection length

UEDGE simulations in simplified slab geometry to study SOL parallel impurity transport for carbon and lithium

- Simulations in slab geometry with NSTX-like plasma parameters:
  - Fixed pitch angle (B_p/B_T~0.1)
  - 12 m midplane-target connection length ~1mm flux surface in NSTX
  - 104 poloidal cells (80 cells from X-point to target), 16 radial cells
- Stronger divertor retention (n_{min}/n_{target}) for lithium than carbon
- Stronger midplane trapping ($n_{midplane}/n_{min}$) for carbon than for lithium
- Divertor retention improved for both carbon and lithium at increased recycling

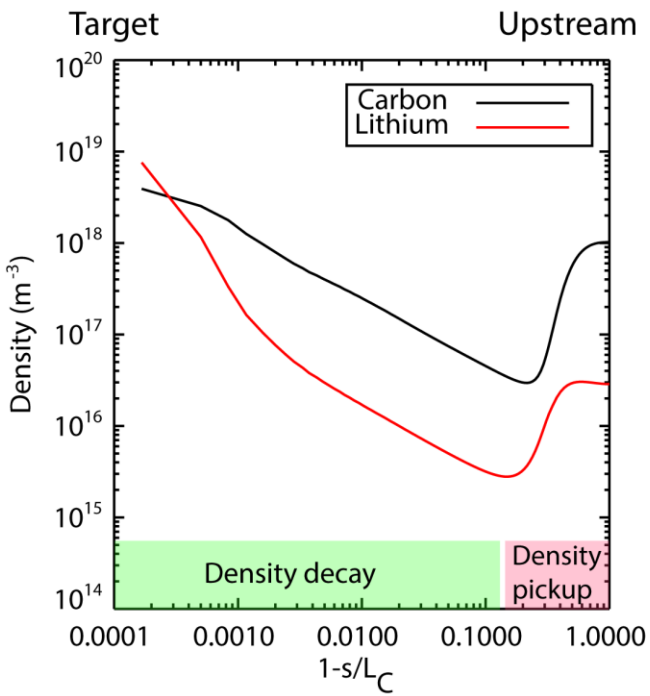

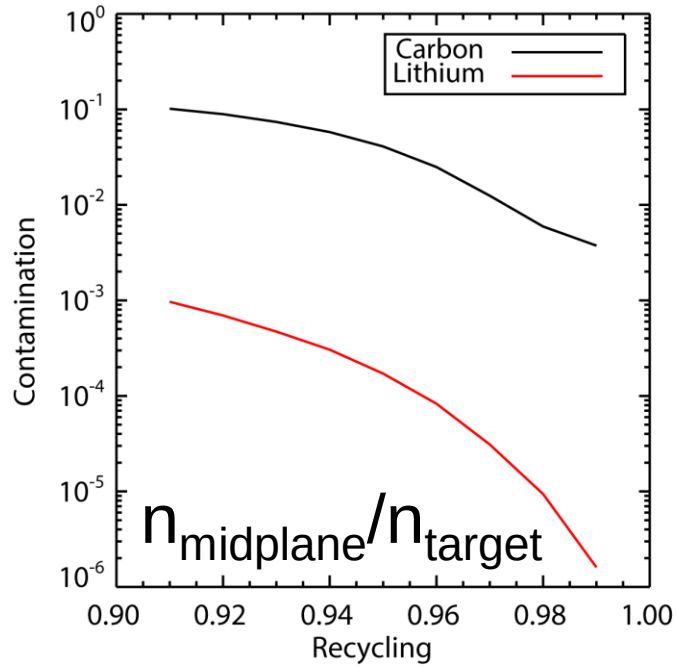

Weaker upstream lithium contamination due to short ionization λ_{mfp} and weaker ∇(Ti) force in slab simulations

Impurity parallel force balance

$$F_z = -\frac{1}{n_z}\frac{dp_z}{ds} + m_z\frac{(v_i - v_z)}{\tau_s} + ZeE + \alpha_e\frac{d(kT_e)}{ds} + \beta_i\frac{d(kT_i)}{ds}$$

∇p_z Force	Friction Force (**FF**)	E-field Force (**FE**)	∇T_e Force (FeG)	∇T_i Force (FiG)

$$F_{eff-j} = m_Z\frac{(v_i)}{\tau_j} + Z_j eE + \alpha_j\frac{\partial T_e}{\partial s} + (\beta_j - 1)\frac{\partial T_i}{\partial s}$$

$$\frac{1}{n_z}\frac{\partial n_z}{\partial s} = \frac{F_{eff}}{T_i} - \frac{1}{D_{eff} n_z}\int_0^s \left(S^0 n_e n_{Z0} - L_\perp\right) ds'$$

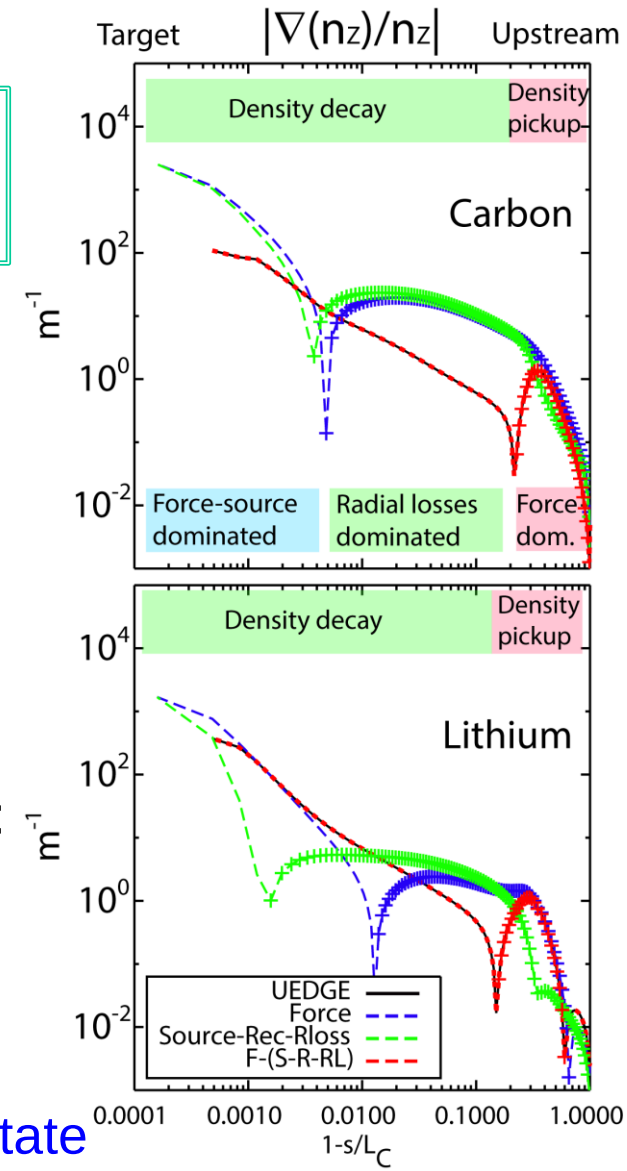

- In density decay region, n_{Li} has larger poloidal drop:
  - Controlled by difference in source profile
- In impurity buildup region n_{Li} has weaker pick-up:
  - In source free region, poloidal density profile controlled by force balance
  - ∇T_i force weaker for lithium due to lower charge state

Core transport analyzed to connect edge sources to core impurity density

Divertor impurity influxes:

- Moderate reduction in carbon sputtering with lithium conditioning
- Lithium sputtering consistent with physical sputtering

SOL parallel transport (UEDGE analysis):

- Stronger divertor retention for lithium than carbon
- Weaker retention at reduced recycling

Core & edge radial transport:

- Carbon:
  - Boronized vs lithiated discharges
- Carbon and lithium
  - Lithiated discharges

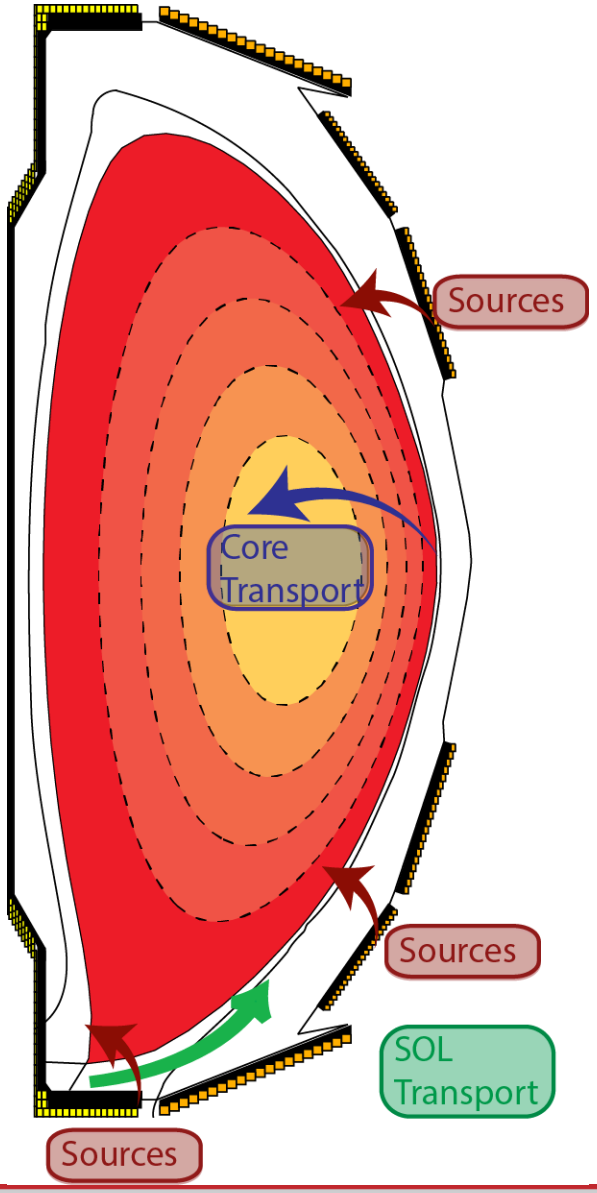

Ion transport found to be close to neoclassical levels in NSTX H-mode NBI-heated discharges

- Ion thermal transport close to neoclassical in NSTX H-modes [Kaye NF 2009]
- Perturbative experiments indicate neon transport close to neoclassical levels:
  - with [Clayton PPCF 2012] and w/o [Delgado NF 2009] lithium conditioning

- Intrinsic impurity transport (carbon, lithium) investigated using:
  - NCLASS [Houlberg PoP 1997]:
    Hirshman-Sigmar formulation based on a fluid-moment approximation
  - NEO [Belli PoP 2009, PoP 2011, PoP 2012]:
    First principles, δ-f code, linearized Fokker-Planck collisional operator
    Includes geometry, rapid toroidal rotation, finite orbit width effects
  - MIST [R. Hulse NTF 1979]:
    Impurity transport code, charge state resolved, D and v input parameters

- In NSTX H-modes, toroidal carbon thermal Mach number often > 1
  - Enhanced transport coefficients
  - Poloidal redistribution of impurity density
  - Asymmetries evaluated with NEO ~ in agreement with experiment [Scotti, NF 2013]

Negligible effect of lithium on carbon transport; lithium neoclassical transport is mostly driven by carbon ions

- Carbon → strong impurity $\left(\alpha_C = \frac{n_C {Z_C}^2}{n_D} \sim 10\right)$, lithium → trace $(\alpha_{Li} \sim 0.1)$
- Pfirsch-Schluter (PS) regime for r/a >0.4 (carbon) and r/a >0.6 (lithium)
- Classical and PS processes can be of comparable importance

- Carbon driven by collisions with D^+, ∇T_D and ∇n_D effects ($\nu_{C\to D} / \nu_{C\to Li} \sim 100$)
- Multi-impurity effects important for lithium ($\nu_{Li\to D} / \nu_{Li\to C} \sim 0.3$)
- In ELM-free, n_C/n_e up to 10%
  - carbon contribution to lithium PS transport dominant
    →10x enhancement in diffusivity

Scan in carbon density

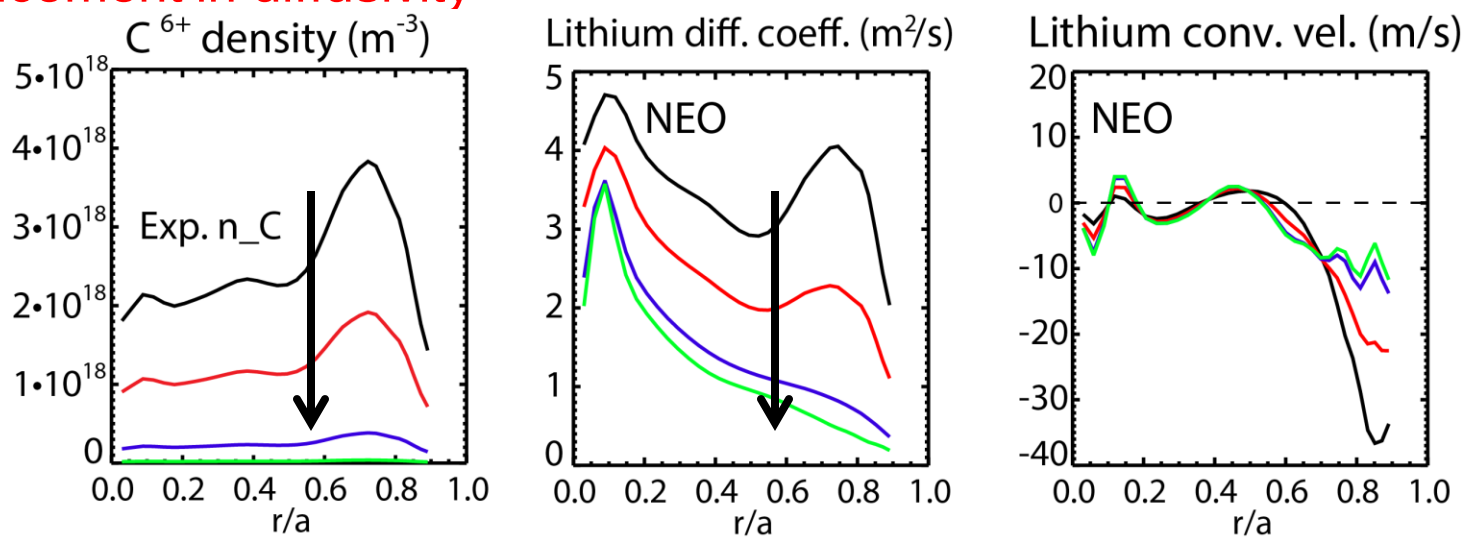

With lithium coatings, changes in deuterium profiles lead to wider carbon inward convection, reduced diffusivity

With lithium conditioning:

- Change in n_D and T_i profiles
  - Wider edge inward convection
  - Increased core inward convection
  - Reduction in edge diffusivity

Carbon PS radial flux

$$\frac{\Gamma^{PS}{}_C}{n_C} = D^{PS}_{C-r}\frac{1}{a}\times\left[\left(-\frac{a}{L_{nC}}\right)+Z\left(\frac{a}{L_{nD}}+\frac{H_{PS}}{K_{PS}}\times\frac{a}{L_{Ti}}\right)\right]$$

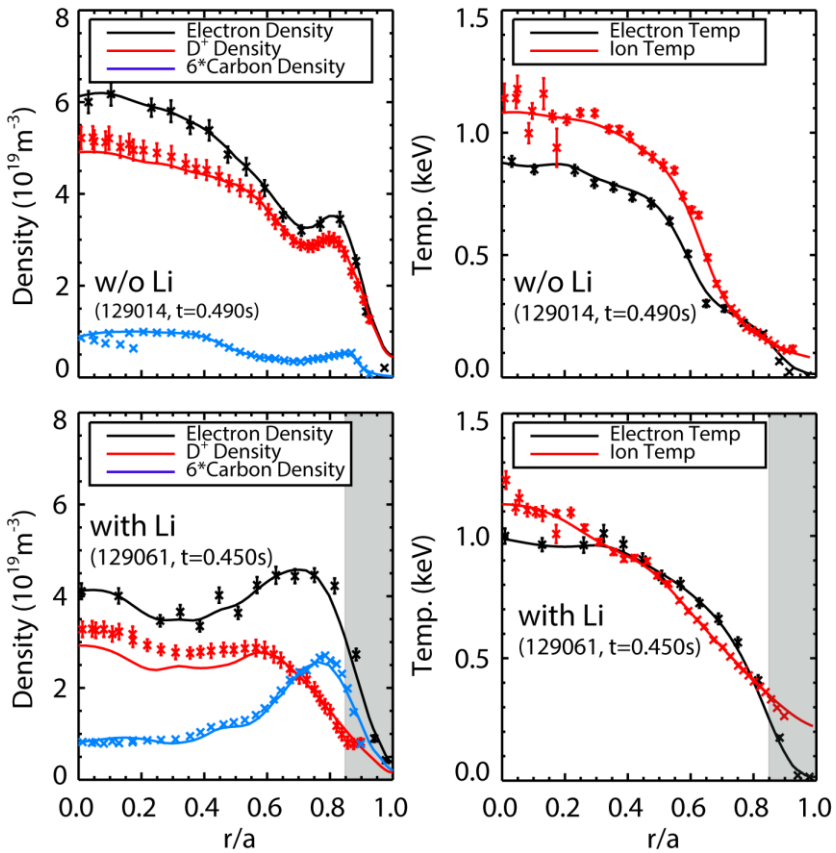

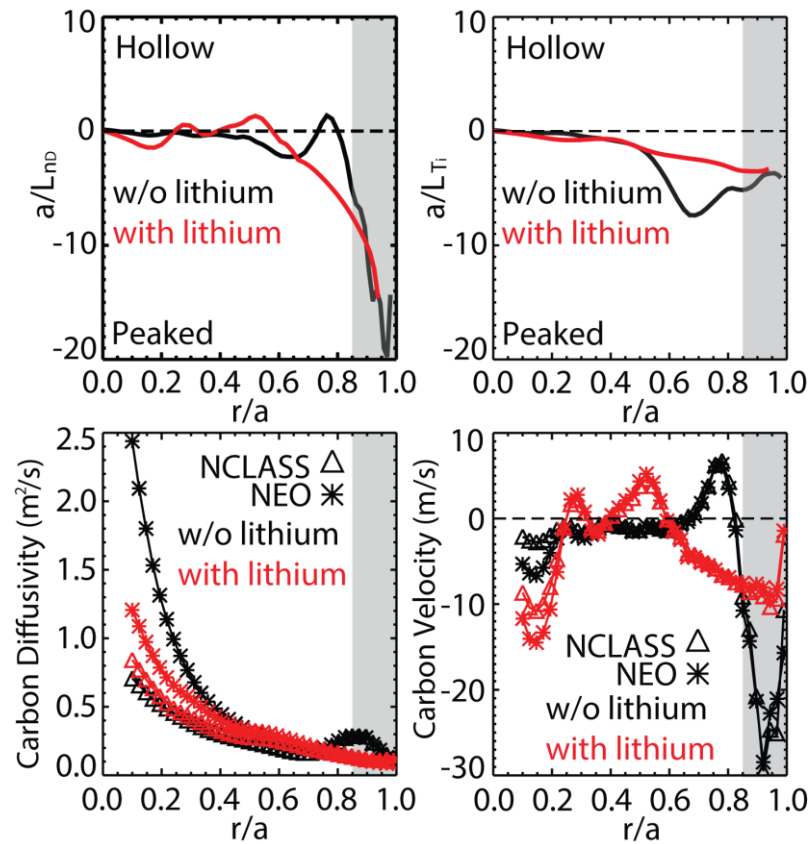

Predictive MIST/NCLASS simulations confirm deviations from neoclassical predictions with lithium conditioning

- MIST simulations
  - Predictive: NCLASS D, v
  - Semi-predictive: NCLASS D, anomalous v
- Without lithium:
  - Agreement in early H-mode
  - Exp. peaking weaker due to ELM flushing
- With lithium:
  - Agreement in early H-mode
  - Stronger edge peaking, but further in than experiment
  - Higher core accumulation (larger than experiment)

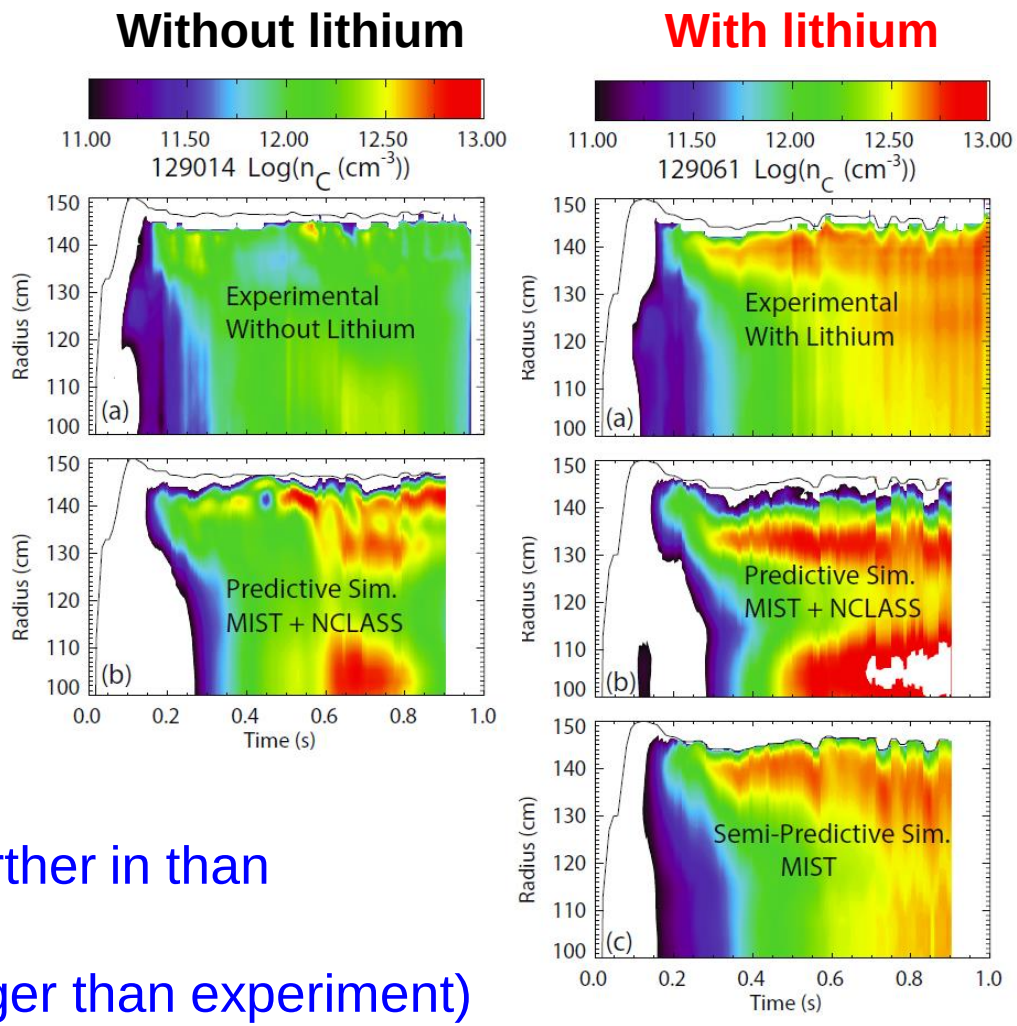

In lithium conditioned discharges residual anomalous transport is needed to explain experimental profiles

- In steady state, source free, peaking $L_{nz}^{-1} \sim v_{exp}/D_{exp}$
- Without lithium, carbon close to neoclassical levels:
  - Weaker edge peaking possibly due to ELM flushing
- With lithium, qualitative agreement:
  - Outward convection region [0.2<r/a<0.6] and edge pinch
- Anomalous outward convection needed at pedestal top
  - Deviations from neoclassical also for ion thermal transport [Kaye,NF2013]

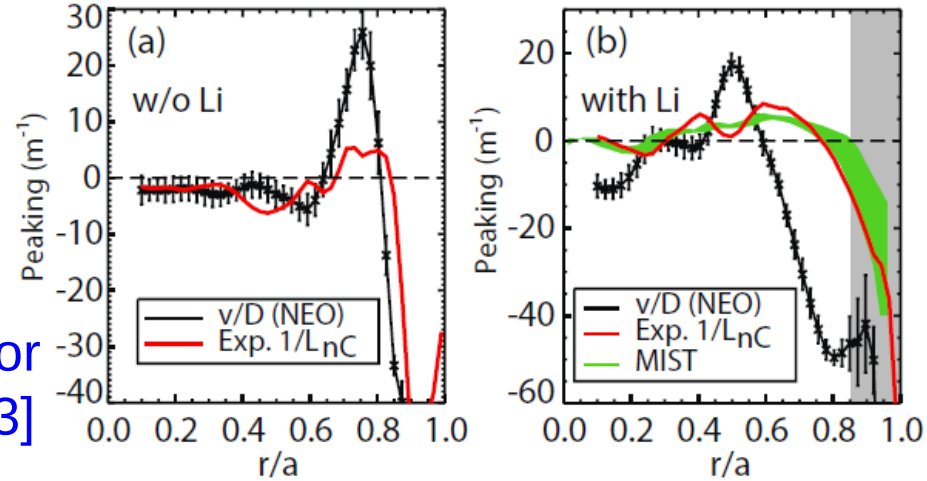

- Assuming neoclassical transport:
  - Different equilibrium n_C profiles
  - Similar core carbon inventories
- Carbon buildup due to disappearance of ELMs with lithium
  - Inventories start deviating at beginning of ELM phase

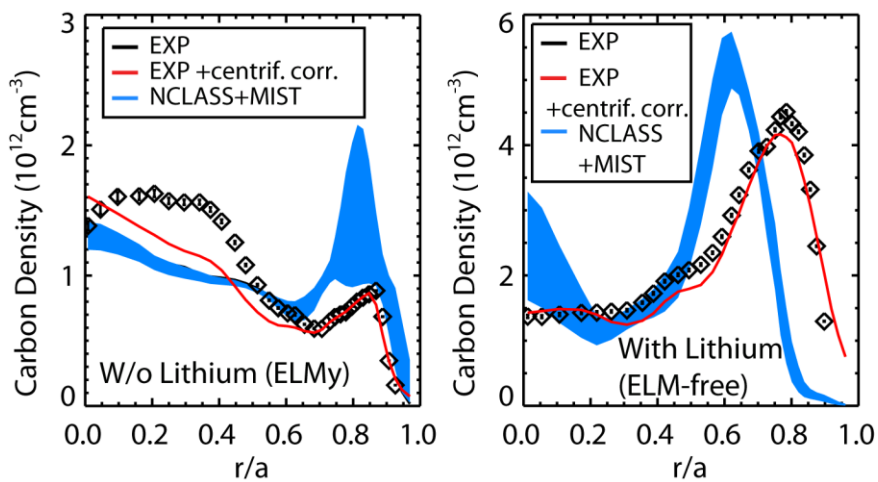

High carbon density leads to increase in lithium diffusivities and is partially responsible for low core lithium densities

- Lithium neoclassical transport mostly driven by carbon ions:
  - High lithium particle diffusivities (D_{Li} ~ 10x D_C)
- Experimental n_{Li} profile shapes agree with neoclassical predictions:
  - High lithium neoclassical level → small role of turbulent transport
- Experimental profiles (n_C, n_{Li}) indicate contribution of edge radial transport to small core n_{Li} (up to 10X):
  - Neoclassical effect is enough to account for this, partially limited by non-neoclassical behavior of carbon
  - Still need source reduction wrt carbon (>10X)

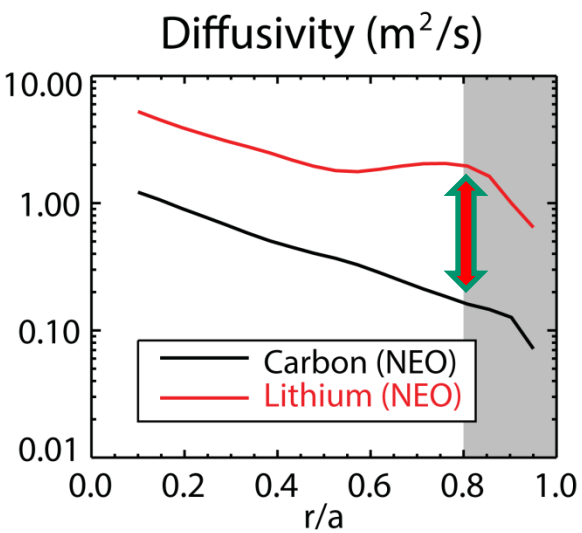

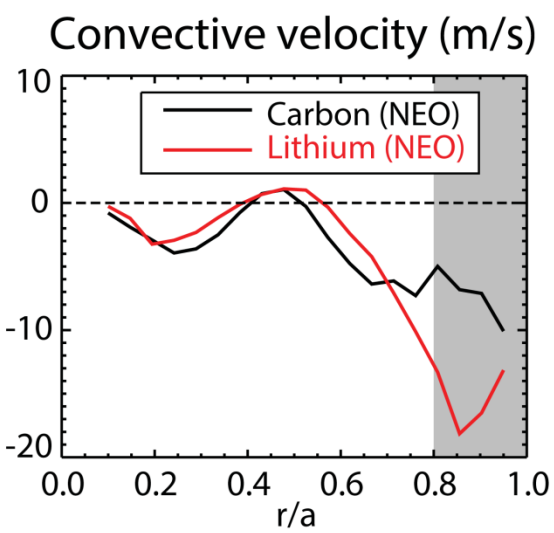

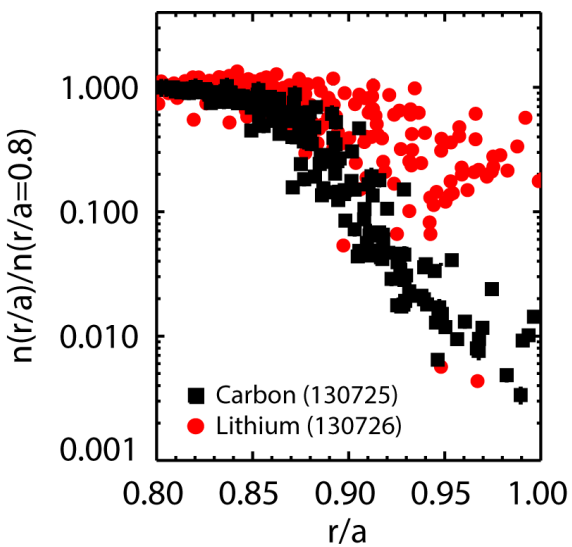

Summary

Divertor influxes from plasma material interaction:

- Moderate reduction in carbon sputtering with lithium conditioning
- Lithium sputtering consistent with physical sputtering

SOL parallel transport (UEDGE modeling):

- Stronger divertor retention for lithium than carbon
- Weaker retention for lower recycling

Core/edge radial transport:

- High neoclassical diffusivity can help prevent lithium accumulation
- Increase in carbon inventories mostly due to disappearance of ELMs

NSTX-U baseline scenario includes lithium-coated graphite PFCs

Several techniques developed in NSTX to limit impurities:

- Triggering of ELMs (3D fields, vertical jogs) [Canik, PRL 2010]
- Source reduction via OSP cooling/detachment (snowflake [Soukhanovskii, PoP 2012], D_2 puff [Scotti, APS 2010])
- Control/moderation of lithium evaporation rate to trigger small ELMs
- Test lithium granule injector for ELM triggering (as demonstrated recently on EAST) [Mansfield NF 2013]